Chapter 1

Introduction

We will start this introduction by giving a short sketch of turbulence: in Section 1.1 we will describe the main features of turbulence (for a complete introduction see [54, 38]), the transition from a laminar flow to a turbulent flow, techniques which are used to simulate turbulence, and some properties of 2D turbulence. In Section 1.2 coherent structures are discussed and techniques to identify coherent structures are described. The ideas and techniques from dynamical systems theory, of which some are used in this thesis, are discussed in Section 1.3.

1.1 Turbulence

Turbulence is one of the great unsolved problems in physics. Little theory is available, and the understanding of turbulence and the transition to turbulence is limited. This is a large problem in the engineering practice, because turbulence plays an important role in many flows. The drag of airplanes and boats would be considerably reduced if the intensity of the turbulence of the flow could be suppressed; the efficiency of pumps could be improved if the turbulence could be controlled; and so on.

What is turbulence? It is hard to give a definition of turbulence. But we can show how a turbulent flow looks like. Fig. 1.1 shows turbulence in so-called Rayleigh-Bernard convection. One can see the irregularity of the flow-pattern. Since a picture can only show a snapshot of a turbulent flow, it is better to think of an unsteady flow. For example everyone has seen the smoke which a smoking person blows out, mostly this flow is turbulent. One can imagine its irregular change in time.

Besides a picture of a turbulent flow we can give some characteristics of a turbulent flow. A turbulent flow has a good mixing property. The large eddy structures present in a turbulent flow transport flow-particles quickly through the whole fluid. A turbulent flow is also highly dissipative. If no energy is added to a turbulent flow, the energy in the flow will decay exponentially. Most of the viscous dissipation takes place at the small scales. This can be made clear with the aid of the Navier-Stokes equations which describe the flow of a fluid. For the case of an incompressible flow, assuming the temperature effects are negligible, they consist of conservation of mass

$$\nabla \cdot \mathbf{u} = 0,$$

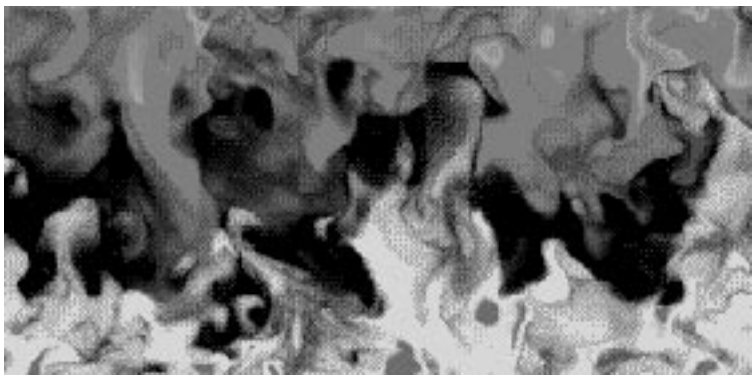

Figure 1.1: *3D Turbulence in Rayleigh-Bernard convection. The top-side is cold, and the bottom-side is heated. Due to the gravity force the flow is unstable. The colors indicate temperature.*

and conservation of momentum

$$\frac{\partial \mathbf{u}}{\partial t} + (\mathbf{u} \cdot \nabla) \cdot \mathbf{u} = -\nabla p + \frac{1}{Re} \Delta \mathbf{u},$$

where $\mathbf{u}$ is the velocity vector and p is the pressure. The equations have been made dimensionless by a length-scale L, determined by the geometry of the flow, and by a characteristic velocity U. The dimensionless parameter Re=UL/ν is the Reynolds number; ν denotes the kinematic viscosity. For large Reynolds numbers, the flow is turbulent. Turbulence occurs in all fluids of which the flow is described by the Navier-Stokes equations, so turbulence is a property of the flow and not of the fluid. In most practical flows Re is rather large ($10^4 - 10^8$), large enough for the flow to be turbulent. A large Reynolds number allows the flow to develop steep gradients locally. The typical length-scale corresponding to these steep gradients can become so small that viscous effects are no longer negligible. So the dissipation takes place at small scales. In this way different length-scales are present in a turbulent flow, which range from L to the Kolmogorov length-scale η. This Kolmogorov length scale is the typical length of the smallest eddy present in a turbulent flow and is determined by dimensional analysis (see [30]). The ratio between the length-scales can be related to the Reynolds number Re, based on the diameter of the largest eddy $\tilde{\mathrm{L}}$ instead of L

$$\frac{\tilde{\mathrm{L}}}{\eta} \propto Re^{3/4}.$$

By the same dimensional analysis the famous Kolmogorov "-5/3" law can be derived. It is derived for homogeneous isotropic turbulence, and states the existence of an exponential decay (with exponent -5/3) of the energy spectrum in the inertial subrange. The inertial subrange is the range where the energy is transported from the scales at which it is produced to the scales at which it is dissipated.

1.1.1 Transition to turbulence

As mentioned in the previous section, for high Reynolds numbers a flow will be turbulent. For small Reynolds numbers the flow will be laminar and stable. Increasing the Reynolds number in a laminar flow will make the flow unstable. This first instability can be analyzed with linear stability theory. An infinitesimal perturbation is superposed on a laminar solution. The signs of the real parts of the eigenvalues of the linearized problem tell whether these disturbances will grow or decay in time. If these disturbances grow in time, the nonlinear terms in the Navier-Stokes equation will come into play. This can result in a globally different flow pattern (like in the Rayleigh-Bernard problem), or a locally different flow pattern (like in a boundary layer). After this first instability the flow is not necessarily time-dependent (like in the Rayleigh-Bernard problem). The first time-dependent flow will be a periodic flow after the first Hopf bifurcation.

What happens if we increase the Reynolds number further, may differ from flow to flow. In only a few cases the transition scenario to turbulence is more or less understood. A few transition scenarios are known in the literature. The oldest one is the Landau route to turbulence (1944). It is based on the idea that after the first periodic solution with frequency ω_1 another instability occurs with a second frequency ω_2, and another with frequency ω_3, and so on. Eventually the energy spectrum will have so much frequencies that it is indistinguishable from a continuous spectrum, and the flow will be turbulent. This scenario has never been observed in experiments and is generally considered to be wrong.

Ruelle and Takens (1972) have proposed another scenario (see [48]). They proved that a dissipative system (like the Navier-Stokes equations) can exhibit chaotic behavior (like turbulence) after the third bifurcation. A simple example of a dissipative system which exhibits such a behavior is given by the set of Lorenz equations. This system is an idealization of the Rayleigh-Bernard problem. A description of the system and its bifurcations can be found in [23].

Another scenario is known as the Feigenbaum cascade (1980) (see [18]). In this scenario the solution undergoes a series of period-doublings, until the bifurcation parameter reaches a critical value where the system has an accumulation point of period-doublings. Feigenbaum also found the convergence behavior of the bifurcation points to the critical value. When the bifurcation parameter passes this point chaos appears. A simple system which has such a behavior is the Duffing equation.

What actually happens in the transition process remains unclear. In a lot of flows the transition process is rather abrupt. This looks like the Ruelle-Takens scenario. In this thesis we will describe the first instabilities for the 2D and 3D flow in a driven cavity by a low-dimensional dynamical system.

1.1.2 Simulation of turbulence

Turbulence would not be such a problem in engineering, if it could be simulated accurately. This is however not possible with the computers available today or in the near future. Direct numerical simulation (DNS), that is resolving all the scales present in a turbulent flow without any modeling, of turbulence is only possible for relatively low Reynolds

numbers. Although DNS is not possible in most practical computations, it can be useful as a mean for obtaining accurate flow data in test problems at low Reynolds numbers. The DNS of the 2D and 3D driven cavity flows in this thesis are performed at Re=22,000 and at Re=10,000. At these Reynolds numbers the flow is only weakly turbulent.

If DNS is not possible the turbulence has to be modeled. Most turbulence models are based on the Reynolds averaged Navier-Stokes equations (RaNS). This approach dates back to previous century. Around 1895 Reynolds decomposed the turbulent flow in a time mean flow and an unsteady fluctuating part. When the Navier-Stokes equations are also averaged in time the result is the Navier-Stokes equations for the mean flow with extra so-called Reynolds stresses. For the incompressible case they are:

$$\tau_{i,j} = \overline{u_i' u_j'}$$

The over-lining means time-averaging, and $u_i^{'}$'s are the fluctuating velocities. These $\tau_{i,j}$'s are not known, so the resulting system is not closed. Therefore, we need extra equations to solve these $\tau_{i,j}$'s. This is the closure problem. For this problem different solutions are used. They can be categorized in four categories, 0-, 1-,and 2-equation models, and second-order closure models.

The 0-equation models, also called algebraic models, are simple models that use an eddy-viscosity hypothesis. The eddy-viscosity hypothesis is based on an assumed similarity between molecular mixing and turbulent mixing. For the definition of the molecular viscosity information of the flow has to be used. If information of the turbulence has to be put into the model they are called incomplete, thus 0-equation models are incomplete. This type of models is widely used, particularly in boundary layers.

In 1-equation models also an equation for the kinetic energy is solved. These models are also incomplete. These models are not very popular, although these models are computationally cheaper than the 2-equation models and second-order closure models.

The most widely used 2-equation model is the k-ϵ model. Along with an equation for the kinetic energy also an equation for the dissipation is solved. 2-equation models are complete, no information of the turbulence has to be put into the model. Another, less popular 2-equation model is the k-ω model (see [61]). In these 2-equation models (and also in the 1-equation model) some closure coefficients have to be fit.

The most complex closure is the second-order closure. In these models no eddy viscosity assumption is made, but for $\tau_{i,j}$ a transport equation is solved. This transport equation introduces new unknowns for which assumptions have to be made. Second-order models are complete. They meet some of the shortcoming of the other models, but they are much more difficult and computationally complex than the other models.

When the Navier-Stokes equations are not averaged in time, but in space with a filter we get a different type of turbulence modeling. Simulation with these kind of models is called large-eddy simulation (LES). The idea behind LES is that the large flow-structures (eddies) have to be computed explicitly, and that the small (subgrid scale) eddies can be modeled because they are more isotropic. In LES we do not have Reynolds stresses, but subgrid stresses. The difference with the RaNS models is that the extra terms in the LES-equations depend only on small scales. Also the LES models are grid dependent whereas the RaNS models are not. The simplest model used for the subgrid stresses is the Smagorinsky model. In this model the subgrid stresses are modeled by

$$\tau_{i,j} = -\overline{u_i^{'}u_j^{'} + u_i^{'}\overline{u_j} + \overline{u_i}u_j^{'}} = 2C_s H^2 \sqrt{S_{i,j}S_{i,j}} S_{i,j}$$

where H is the filter width. The over-lining means space averaging. The mean strain-rate tensor $S_{i,j}$ is defined as

$$S_{i,j} = \frac{1}{2}(\frac{\partial \overline{u_i}}{\partial x_j} + \frac{\partial \overline{u_j}}{\partial x_i}).$$

Just like in the 0-, 1- , and 2-equation models for RaNS, the assumption is made that the eddy-viscosity is similar to the molecular viscosity. This eddy viscosity is taken constant over the whole flow-domain. A more recent development are the dynamical subgrid models. In these models two filters are used to replace the Smagorinsky constant by a space dependent variable.

1.1.3 2D turbulence

Turbulence is a three dimensional feature. Nevertheless we can speak of turbulence in two spatial dimensions, but the characteristics are different from three dimensional turbulence. 2D turbulence can be seen on weather maps where large 2D high and low-pressure areas determine the large scale behavior of the weather system. It can also be seen in rotating flows and in the flow of stable stratified fluids where velocity fluctuations in the third dimension are damped.

An important characteristic of (3D) turbulence which we didn't mention in previous sections is the high level of vorticity fluctuations. Vorticity is the rotation or curl of the velocity field:

$$\boldsymbol{\omega} = \nabla \times \mathbf{u}.$$

In 3D turbulence, vortex stretching is an important mechanism, by which energy is transported from the large scales to the small scales. Vortex stretching is caused by a non-zero velocity component in the direction of the axis of a vortex-tube. Due to this velocity component the vortex-tube will become longer and thinner and the level of vorticity will increase. This process is not possible in 2D turbulence, because the axis of a vortex-tube and the velocity are always orthogonal. Therefore, 2D turbulence lacks this mechanism of transporting energy from the large to the small scales.

A typical feature for 2D turbulence is self-organization, which is transport from small scales to large scales; this is also called the inverse kinetic energy cascade. Important quantities for describing this mechanism are the energy E and enstrophy Q;

$$E = ||\mathbf{u}||^2, \qquad Q = ||\nabla \times \mathbf{u}||^2.$$

In the absence of frictional forces (we do not consider the smallest dissipative scales) the total energy and total enstrophy are conserved. In spectral terms the enstrophy is k^2 times the energy, where k is the wavenumber,

$$Q(k) = k^2 E(k).$$

If both quantities are conserved, more energy has to go to the small wave-numbers, i.e. to the large scales. The enstrophy, on the other hand, will move to the higher wave numbers. The result is that, if no energy is added to a 2D turbulent flow, the vortex structures in 2D turbulence become larger and larger, and the vorticity will be concentrated in a thin layer at the edge of the vortex structures. Because a 2D turbulent flow is weakly dissipative the vortex structures will exist for a long time. These properties together result in the self-organizing property of 2D turbulence.

An example of this can be seen in Fig. 1.2. In the 2D flow around the square cylinder the small scale structures at the edge of the square cylinder become more and more organized when they are moving further away from the square cylinder. The vortex structures which we can see are mono-, di-, and tripole vortices.

Figure 1.2: *Vorticity of a 2D turbulent flow around a square cylinder at* $Re = 10,000$ *(from [62]). Mono-, di-, and tri-pole vortices are present. Light gray colors indicate positive vorticity, and dark gray colors indicate negative vorticity.*

Just like the "-5/3" law for 3D homogeneous isotropic turbulence, 2D homogeneous isotropic turbulence has an exponential decay of the energy spectrum in the inertial subrange. The exponent in 2D is -3.

The 2D turbulent flow simulated in this thesis, the 2D driven cavity, has, due to the geometry, a constant accumulation of energy on the small scales. The self-organizing property can be observed when an eddy-structure enters the core region of the cavity. Such an eddy-structure exists for a relative long time and has the form of a di-pole (see Fig. 3.11).

1.2 Coherent structures

A property of a turbulent flow is its irregularity. Despite this irregular flow-pattern turbulent flows are known to possess coherent structures. Coherent structures are recognizable flow-structures which survive dissipation for a relatively long time, frequently re-appear and possess a typical life-cycle. Coherent structures are known since the fifties and subject to a lot of research. If the dynamics of these coherent structures is better understood this knowledge can be used to improve turbulence models. On the other hand, in engineering practice, people are interested in the suppression of the development of these structures

since suppression of development can lead to drag-reduction, e.g. In this context one can think of ribblets, i.e. small-scale profiles on for example boats which reduce the drag at certain boat-velocities.

A well-known example of coherent structures are the hairpin vortices which appear in a turbulent boundary layer. These are vortex structures which look like hairpins. They move from very close to the boundary into the turbulent boundary layer. Much of the turbulence production near the boundary is associated with this process which is called bursting.

Another example are the eddy-structures in a free shear flow. These eddy-structures originate in the transitional part of the shear layer. They pair and grow in the downstream direction.

Various techniques are used to make the coherent structures visible. The most straightforward way is flow visualization of any kind. This can be visualization of experiments or numerical simulations. Also a lot of mathematical techniques are used to identify the coherent structures: for example Fourier transforms, conditional sampling, stochastic estimation, wavelet transforms, and the proper orthogonal decomposition (POD). Here we will describe two of these techniques, conditional sampling and stochastic estimation. POD is described in Chapter 2.

Conditional sampling is a widely used method to identify coherent structures. The method consists of a conditional averaging over a set of flowfields. So, the method requires some a priori knowledge of the coherent structures to determine the condition used in the conditional sampling. This is a major drawback of the method, because it is not an objective method. The condition can be chosen such that one sees what one wants to see, with the possibility of missing important flow features.

Stochastic estimation does not require a condition. Stochastic estimation is the estimation of random variables as a function of other random variables which are known. For a coherent structure this is the estimation of a velocity field $u = u(x,t)$ given the velocity field at certain points in space and time $u_{ij} = u(x_i, t_j)$. The best estimate in mean square sense is the conditional average of u given u_{ij}: $< u|u_{ij} >$. If u and u_{ij} are joint normally distributed this is a linear function of u_{ij}. With this assumption it is called linear stochastic estimation.

Under certain conditions it can be shown (see [8]) that linear stochastic estimation is the same as POD. In this thesis we used POD because of its mathematical properties and its optimal energy content which gives rise to the expectation that it is sufficient to use only a relatively low number of POD eigenfunctions in a dynamical system.

1.3 Turbulence and dynamical systems

There has been a growing interest in dynamical systems theory in the turbulence research community over the last decades. A stimulus in this direction was the suggestion of Ruelle and Takens in 1971 [48] that turbulence takes place on a strange attractor. A popular example is the Lorenz attractor.

The attractor of a (dissipative) dynamical system is a subset of the state-space which attracts all solutions and is invariant under the dynamical system. That means that an

arbitrary point of the state-space will converge to the attractor if time evolves and a point on the attractor will stay on the attractor for all time. The attractor can be for example a single point, a limit cycle, a torus of dimension 2 or higher, or a strange attractor.

The difference between a normal and a strange attractor is that a strange attractor contains a chaotic invariant set. A chaotic invariant set has a complex structure and looks locally like the product of a manifold and a Cantor set. Solutions on the chaotic set have the property that they possess sensitive dependence on initial conditions. This means that two solutions starting arbitrary close to each other will diverge exponentially fast from each other in time.

There are different types of characterizations of strange attractors. A straightforward way is to compute a solution on the strange attractor and compute its power spectrum. A broad band in the power spectrum will characterize a strange attractor. Peaks in the power spectrum will indicate characteristic frequencies of the dynamical system.

Another characteristic of a strange attractor, denoted by A, is a positive Liapunov exponent. A Liapunov exponent is a measure of the average exponential divergence of nearby trajectories. The Liapunov exponents L_i of a dynamical system with solution $\boldsymbol{a}(\boldsymbol{x}, t)$ at point $\boldsymbol{x}$ of the attractor, can be defined with the aid of the basisvectors $\boldsymbol{e}_i(\boldsymbol{x})$ of the tangent space $T_{\boldsymbol{x}}A$

$$L_i(\boldsymbol{x}) = \lim_{t\to\infty} \frac{1}{t} \ln \frac{||\mathrm{d}\boldsymbol{a}(\boldsymbol{e}_i(\boldsymbol{x}), t)||}{||\boldsymbol{e}_i(\boldsymbol{x})||}$$

where $\mathrm{d}\boldsymbol{a}$ is the Jacobian of $\boldsymbol{a}$. The Liapunov exponents have the same value for almost all $\boldsymbol{x}$. If at least one of the L_i's is positive the attractor is chaotic.

A chaotic set can also be characterized by a fractional Hausdorff dimension. The Hausdorff dimension d of a set A is defined in the following way. Suppose we have a collection of sets U_i of maximum diameter δ which covers A. Given a number α we can define d^α

$$d^\alpha = \lim_{\delta\to 0} \sum_{i=1}^{\infty} (diam(U_i))^\alpha$$

To illustrate what this means we give the following example. For a unit flat square S in $\mathbf{R}^3$ we have $d^1 = \text{length}(S) = \infty$, $d^2 = \text{area}(S) = 1$, and $d^3 = \text{volume}(S) = 0$. If we now take for d the infimum of α such that $d^\alpha = 0$, we obtain for "normal" sets just what we would like to call the dimension and chaotic sets are characterized by a fractal Hausdorff dimension. The Hausdorff dimension is a measure of the relative volume of A in the embedded space.

In dynamical systems theory a lot of research has been done on systems with 3 or 4 degrees of freedom. Even in a weakly turbulent flow the number of degrees of freedom is often in the order of 10 to 100. Therefore direct application of results of dynamical systems theory to turbulent flows is not possible, or very difficult. With the aid of time-series analysis it is possible to compute an estimate of the number of the degrees of freedom of a turbulent flow.

In the early stages of transition, i.e. when steady, periodic or quasi-periodic flow can be observed, it is possible to get a global description of the dynamical behavior of the

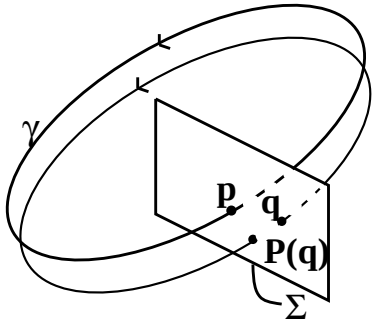

Figure 1.3: *The Poincaré map with hypersurface* Σ

flow. In the Chapters 5 and 7 we will use some techniques to determine the stability of steady and periodic solutions of a dynamical system. These techniques will be described here for the following dynamical system:

$$\frac{\mathrm{d}\boldsymbol{a}}{\mathrm{d}t} = \mathbf{f}(\boldsymbol{a}, Re),$$

The Reynolds number Re is the bifurcation parameter. Suppose we have a steady solution $\boldsymbol{a}^0$, then

$$\mathbf{f}(\boldsymbol{a}^0, Re) = 0.$$

This solution will be stable if the Jacobian of the linearized system

$$\frac{\mathrm{d}\boldsymbol{a}}{\mathrm{d}t} = \mathbf{J}(\boldsymbol{a}, Re)\boldsymbol{a}, \qquad \mathbf{J}_{i,j} = \{\frac{\partial f_i}{\partial a_j}\} \tag{1.1}$$

possesses no eigenvalues with a positive real part. The solution $\boldsymbol{a}^0$ becomes unstable if an eigenvalue crosses the imaginary axis. When one eigenvalue crosses the imaginary axis it necessarily crosses through the origin. Generally the solution after such a bifurcation is steady again. When it is a degenerate eigenvalue, however, the situation can be very complex. For our dynamical system we will encounter only a pair of complex conjugate eigenvalues, $\lambda + i\omega$, crossing the imaginary axis, which corresponds to a Hopf bifurcation. The solution after such a bifurcation will normally be periodic with period $2\pi/\omega$.

For the stability of the periodic solution we will consider the *Poincaré map* P. Suppose we have a periodic orbit γ. We take a cross section Σ. The dimension of this hypersurface is one less than the dimension of the state space. The solutions have to be transverse to Σ. The periodic solution intersects Σ in only one point p. The *Poincaré map* P maps points q of Σ in some neighborhood $U \subset \Sigma$ of p by following the solution through q until it first crosses Σ again. It is also called the *first return map* (see Fig. 1.3).

The periodic orbit γ is stable if all points q in U converge to p under the iteration of P. To determine whether γ is stable we need to compute the linearization $\mathrm{D}P$ of the map P at p; γ is stable if the eigenvalues of $\mathrm{D}P(p)$ have norm less than one. To derive an expression for $\mathrm{D}P$ we have to linearize the dynamical system along the periodic orbit γ with solution $\boldsymbol{a}^1(\boldsymbol{x})$

$$\frac{\mathrm{d}\boldsymbol{b}}{\mathrm{d}t} = \mathbf{J}(\boldsymbol{a}^1(\boldsymbol{x}), Re)\boldsymbol{b} \tag{1.2}$$

If we integrate this linearized system along γ over the period T of solution $\boldsymbol{a}^1(\boldsymbol{x})$ we obtain an expression for $\mathrm{D}P$ which reads

$$\mathrm{D}P = e^{\int_T \mathbf{J}(\boldsymbol{a}^1(\boldsymbol{x}), Re)\mathrm{d}t} \tag{1.3}$$

The eigenvalues of $\mathrm{D}P$ are called *Floquet multipliers*. If one or more Floquet multiplier(s) cross(es) the unit circle in the complex plane when the Reynolds number is varied the periodic solution will become unstable. In our case the right-hand side $\mathbf{f}$ does depend explicitly on the time t, so the starting point $\boldsymbol{x}$ can be chosen arbitrary along the solution. Therefore we always find a Floquet multiplier +1. This Floquet multiplier does not have to be considered in the bifurcation analysis. The solution after the bifurcation depends on the position along the unit circle where the Floquet multiplier(s) cross(es) the unit circle.

If a Floquet multiplier crosses the unit circle at +1 we get two periodic solutions after the bifurcation; one is attracting and one is repelling.

If a Floquet multiplier crosses the unit circle at -1 a period doubling appears, and the Floquet multipliers of the new solution will be squares of the Floquet multipliers of the old solution.

If a pair of complex conjugate eigenvalues, $\lambda \pm i\mu$ (with $\mu \neq 0$) crosses the unit circle the solution after the bifurcation will be periodic or quasi-periodic. It will be periodic if there are integers n and m such that $m\mu = 2n\pi$. Then the attractor is an orbit on a 2-torus. If there are no n and m such that $m\mu = 2n\pi$ holds, the solution will be quasi-periodic and the attractor will be a 2-torus. In our case it is not possible to make a distinction between periodic and quasi-periodic because we can only approximate the Floquet multipliers. For small n and m it is possible to see the periodic behavior in a phase-plot.